

Regular Undulation Morphology Observed on Fracture and Film Surfaces of Chiral S_C^* Polymer

Chunying Zhang, Susumu Edo, Ryouhei Ishige, Masatoshi Tokita, and Junji Watanabe*

Department of Organic and Polymeric Materials, Tokyo Institute of Technology, Ookayama, Meguro-ku, Tokyo 152-8552, Japan

Received March 7, 2008; Revised Manuscript Received May 21, 2008

ABSTRACT: The chiral smectic C^* (S_C^*) solid was prepared from the main-chain type of liquid crystal polymer, and its surface morphologies on the fracture and film surfaces were studied by SEM and AFM observations. Very clear undulation with a regular repeating can be detected by both methods. The peak to peak distance corresponds to the helical pitch of chiral S_C^* phase, and the depth from top to bottom is 10–15% and 2–3% of the pitch length for the fracture and film surfaces, respectively. Such a distinct undulation morphology results from the helical arrangement of polymers which are incorporated into the macrohelix of S_C^* . This study shows that the inner nanostructure can induce the surface nanostructuring which could be applied to the optical devices.

Introduction

Chiral smectic C (S_C^*) liquid crystal (LC) is one of the most fantastic LC phases since it exhibits the ferroelectric response and forms the helical structure.¹ Especially, the helical structure has been attracted from its characteristic optical properties, huge optical rotation, and selective reflection of the circularly polarized light, which can be applied to optical materials. By these reasons, the chiral S_C^* phase has been extensively studied in the low-molecular-weight molecular system. The chiral S_C^* LC is also formed from the main-chain type of polymers with the mesogenic groups linked by the aliphatic spacer.^{2,3} In this polymer system, the mesogenic groups participate to form the smectic layer so that the polymers themselves form the helical conformation to conform to the helical LC field (see later in Figure 3). This situation is completely different from that in the low-molecular-weight system where each molecule participates in each layer. In this article, we report that the characteristic undulation morphology is observed on the fracture surface of the glassy S_C^* LC because of the helical association of polymer molecules. The peak to peak distance of undulation corresponds to the helical pitch of chiral S_C^* phase (150–600 nm depending on the chiral content in polymers), and the depth of the undulation is around 20–80 nm. A preferential cleavage along the helical polymer chain is considered to create such an undulation surface. Together with the easy preparation of wide-area monodomain, polymeric S_C^* phase provides the powerful way to fabricate the surface undulation which can be applied to the diffraction grating.

Experimental Section

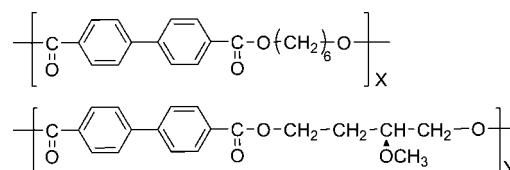
Preparation. The polyesters were synthesized by melt condensation of dimethyl-4,4'-biphenyl dicarboxylate, 2-methoxy-1,4-butanediol, and 1,6-hexanediol with isopropyl titanate as catalyst. The molecular weight (M_w) was determined from gel permeation chromatography (GPC) in chloroform solution on the basis of calibration of standard polystyrene.

Measurement. AFM images were taken with an Agilent Series 5500 atomic force microscope. Imaging was conducted in tapping mode using a silicon cantilever with a resonance frequency of 75 kHz. FE-SEM images were obtained with a JEOL JSM-7500F field emission scanning electron microscope. For this measurement, a Pt/Pd layer (thickness ~ 2 nm) was deposited onto a surface of the sample using a HITACHI E1030 ion sputter. X-ray patterns were

recorded on an imaging plate with a Rigaku RU200BH (Ni-filtered Cu $K\alpha$ beam).

Results and Discussion

The S_C phase treated here is formed from the following main-chain type of BB- n copolymers



which are composed of bibenzoate mesogen and two flexible spacers of hexamethylene (HM) and 2-methoxybutylene (MOB) groups. Homopolymer BB-6 with HM spacer forms a S_A phase,⁴

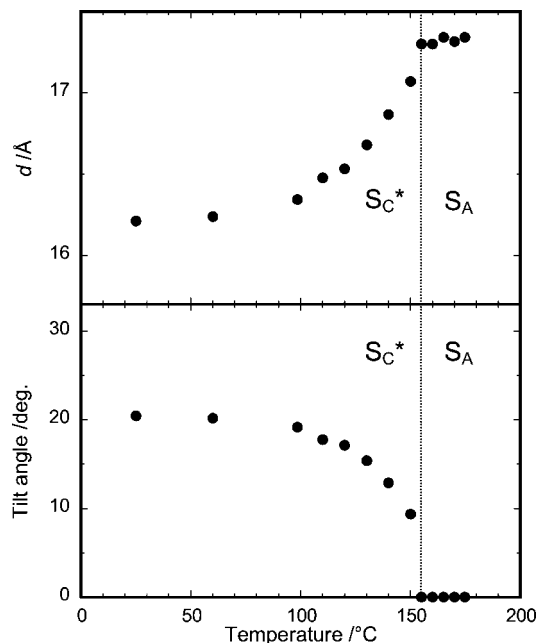


Figure 1. Temperature dependence of (a) the smectic layer spacing and (b) the tilt angle observed for BB-40/60(100). In (b), the tilt angle was calculated from the layer spacing under the assumption that the averaged conformation of polymer chain remains unchanged on phase transition from S_A to S_C^* .

* Corresponding author. E-mail: jwatanab@polymer.titech.ac.jp.

Table 1. Repeating Length L and Height H of the Sinusoidal Undulation Observed on the Fracture and Film Surfaces of Polymeric Chiral S_C^* Solids with Various Helical Pitches

copolymer	$M_w \times 10^{-3}^a$	helical pitch P/nm^b	fracture surface			film surface	
			SEM	AFM		AFM	
			L/nm	L/nm	H/nm	L/nm	H/nm
P-40/60(100)	5.5	177	155–170	172–180	19–21	195–215	4.0–5.5
P-40/60(80)	6.0	214	215–230	210–230	23–28	235–255	4.5–6.5
P-40/60(50)	4.4	304	255–295	280–300	35–45	315–340	7.5–9.5
P-40/60(35)	4.1	591	545–595	580–600	70–80	550–605	8.0–11.5
P-40/60(0)	6.1	∞					

^a Elucidated from GPC in chloroform solution on the basis of calibration of standard polystyrene. ^b Determined from the wavelength of full-pitch (or half-pitch) reflection band, λ , by using the equation $\lambda = 2nP$ (or $\lambda = nP$), where n is 1.5.^{2,6}

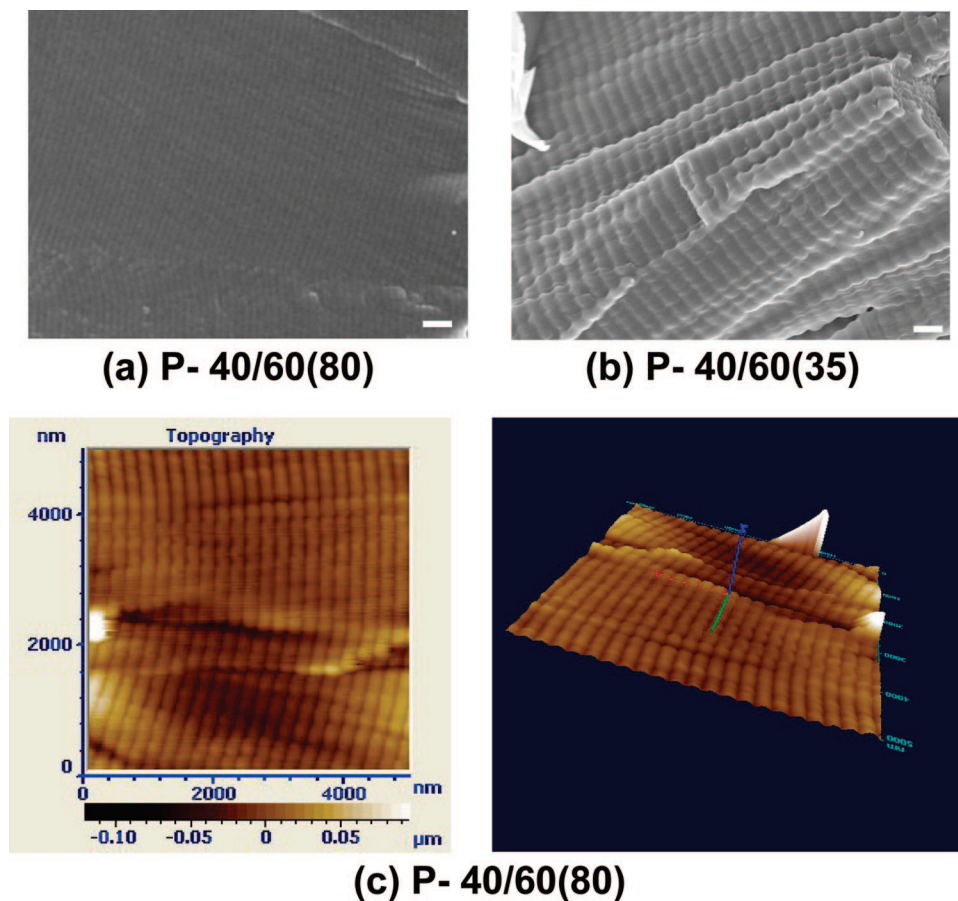
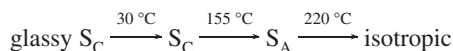


Figure 2. FE-SEM images observed on the fracture surface of (a) of BB-40/60(80) and (b) BB-40/60(21). The length of the bar is 1 μm . (c) is AFM image for the same sample in (a).

whereas homopolymer BB-4(2-MeO) with MOB spacer forms nematic and S_C phases.⁵ The incorporation of the BB-4(2-MeO) unit into BB-6 polymer results in an alteration of S_A to S_C phase,^{2,3} indicating that the methyl or methoxy substitution into the spacer group induces the tilting of mesogens to the layer. Thus, the copolymers with intermediate contents of 40–60% show the polymorphism of mesophases: isotropic, S_A , and S_C phases in order of decreasing temperature. Further, as we know, the copolymerization interrupts the crystallization of liquid crystal, and then the lowest temperature S_C phase can be solidified without crystallization on cooling. These glassy solids are convenient for an examination on the fracture surface morphology. Herein, we use the copolymer with 60% content of MOB. The transition behavior of this copolymer is as follows:



The MOB group has an asymmetric carbon so that the use of chiral (*S*)-MOB or (*R*)-MOB leads to the formation of chiral

S_C^* phase. Helical twisting power is adjusted by the chiral content which is defined here as a molar ratio of ((*S*)-MOB – (*R*)-MOB) to ((*S*)-MOB + (*R*)-MOB)). The polymers are named as P-40/60(*X*), where 40/60 indicates the molar ratio of BB-6 to BB-4(2-MeO) unit and *X* the percent chiral content of MOB group which is varied from 0 to 100%. In Table 1, the used copolymers are listed together with their molecular weights.

In these copolymers, the transition of S_A to S_C^* can be detected from DSC and optical microscopic methods, but it is more definitely detected from an estimation of layer spacing by X-ray method; the layer spacing of the S_C^* phase is relatively smaller than that of the S_A phase since in the S_C^* phase molecules are tilted to the layer.^{2,3} Tilt angle can be calculated from a relative ratio of the spacing of S_C^* to that (1.73 nm) of S_A phase. Figure 1 shows the temperature dependence of layer spacing and tilt angle for the S_A and S_C^* phases as observed in P-40/60(100). The tilt angle increases from 0 to 20° as the temperature decreases. At a glassy state of S_C^* phase, hence, the tilt angle is around 20°.

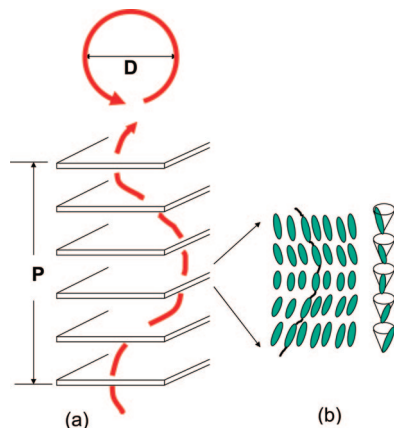


Figure 3. (a) Schematic representation of main-chain LC polymer running through the helically aligned S_C^* layers. To allow the c -director rotation of mesogenic groups as in (b), the polymer has to assume the helical conformation. The polymer in (a) is illustrated with a molecular length long over the pitch, although the real length of the used polymer is more or less than 50 nm.

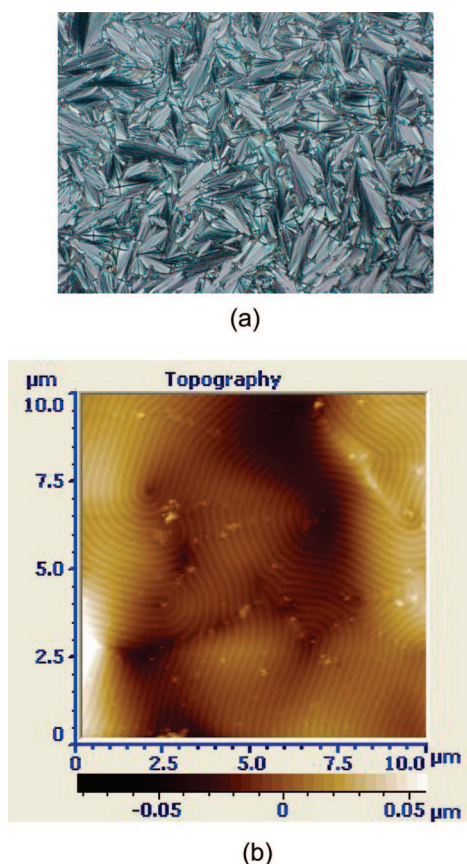


Figure 4. (a) Optical microscopic fan-shaped texture and (b) its AFM image of the film surface in S_C^* solid film of BB-40/60(80) coated on a glass substrate.

Helical pitches (P) of S_C^* phase were determined for the homeotropically aligned film with the helical axis perpendicular to the film surface, which can be prepared by shearing between two glass plates. The determined pitches at room temperature are listed for the copolymers with various chiral contents in Table 1. One can find the conventional trend that the twisting power ($1/P$) is proportional to the chiral content, X .

To prepare the chiral S_C^* solid with the well-developed helical structure, the bulk polymer is heated up to the S_A temperature of 180 °C and then cooled down to the chiral S_C^* phase at a rate of 1 °C min⁻¹. Formation of the helical structure in the S_C^* can be

recognized from an exhibition of opal-like reflection colors. The S_C^* solid is then immersed into liquid nitrogen and fractured by giving a crack with knife. The fracture surface was coated with a Pt/Pd layer by vacuum sputtering. The morphologies were photographed by field emission scanning electron microscopy (FE-SEM). Parts a and b of Figure 2 show the FE-SEM images observed for P-40/60(80) and P-40/60(35), respectively. As observed here, the regularly repeated stripes with black and white contrast are detected for all the chiral S_C^* samples. The repeat length (L) decreases as the chiral content increases. These black and white stripes can be explained to result from the undulation structure with peaks and valleys (i.e., a series of parallel grooves). In fact, such an undulation mode is found in some parts where a beam is accidentally irradiated parallel to the fracture surface (see Figure 2b). The undulation takes place sinusoidally, and its height (H) from the top to peak is estimated as around 80 nm from Figure 2b. The AFM image also shows the similar undulation structure in Figure 2c, allowing the direct estimation of H . The values of L and H estimated from FE-SEM and AFM images are listed in Table 1 and compared with the helical pitches determined from spectroscopic methods. Obviously, L corresponds to the pitch of chiral S_C^* helical structure in all of the copolymers with different chiral contents. It should be noted that the nonchiral S_C solid in P-40/60(0) does not produce the undulation surface, but the flat surface.

Such a sinusoidal undulation can be explained to arise from the polymeric effect. As stated above, in the main-chain polymer system each repeating mesogenic unit (bibenzoate unit) participates into each layer.⁴ By this reason, the polymer runs through many layers. In the S_A phase, the polymers themselves lie perpendicular to the layer as the mesogenic units do, while in the S_C phase, they are tilted to the layer normal with the certain tilt angle depending on the temperature.^{2,3} In the chiral S_C^* phase, in addition, the tilt direction of mesogenic groups, i.e. c -director, rotates to result in the helical structure around the layer normal. In other words, the polymer chain assumes the helical conformation when it goes up from the layer to layer, which is schematically illustrated in Figure 3.

Diameter (D) of the helical conformation is related to the helical pitch (P) which is determined from the full- and half-pitch reflection spectra^{2,6} observed on the homeotropically aligned S_C^* . With the length of repeating unit, l (corresponding to the layer spacing in S_A), tilt angle, θ , and the number of layers, m , included in one pitch, P can be given by

$$P = ml \cos \theta \quad (1)$$

On the other hand, D is approximated by the relation

$$D \approx ml \sin \theta / \pi \quad (2)$$

Hence

$$D/P = \tan \theta / \pi \quad (3)$$

In the present S_C^* solid, l is 1.73 nm and θ is 20°, leading to $D/P = 0.12$. Thus, one knows that polymers assume the gentle helical conformation; for example, the helical conformation with $P = 590$ nm and $D = 71$ nm for P-40/60(35) polymer. In such a S_C^* helical solid, the cleavage may easily occur along the helical polymer, since the polymers are laterally associated with a weak van der Waals force. Such a preferential cleavage results in the undulation morphology on fracture surface (refer to Figure 3). D/P should correspond to H/L . This is just recognized from Table 1.

Of interest is to know how the sinusoidal undulation is produced on the film surface of homogeneously aligned chiral S_C^* film coated on a glass substrate. Parts a and b of Figure 4 show the optical microscopic fan-shaped texture of the chiral S_C^* phase and the AFM image from its film surface, respectively. Similarly as in the fracture surface, AFM image shows the undulation

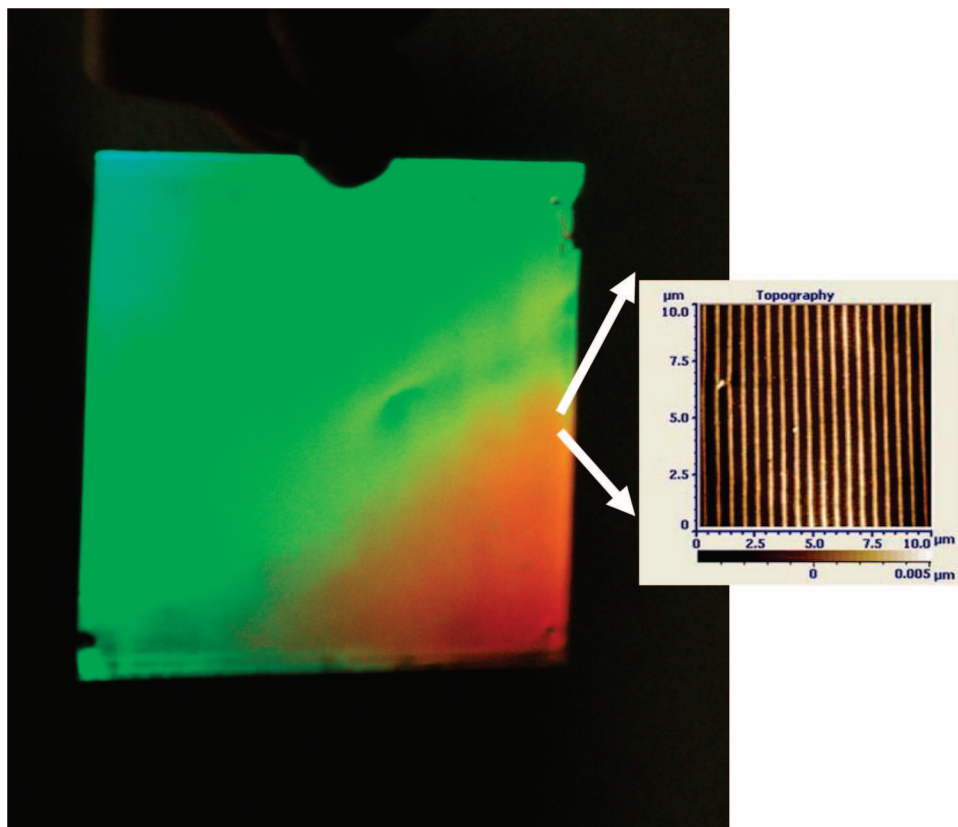


Figure 5. Reflection color from the homogeneous monodomain S_C^* film of BB-40/60(35) with a area size of $20 \times 20 \text{ cm}^2$ and a thickness of $5 \mu\text{m}$, which was prepared on a rubbed substrate. As observed in AFM image (see inset), such a monodomain film gives equally spaced grooves perfectly aligned perpendicularly to the rubbing direction.

structure. Its polygonal alignment is expected from the optical microscopic fan-shaped texture.⁷ L corresponds to the helical pitch; however H , less than 10 nm , is fairly smaller than those observed on the fracture surface (see Table 1). Probably, the interfacial tension may force to produce the more smooth undulation.

Noteworthy is that the chiral S_C^* film can be prepared with the homogeneous monodomain structure over a sample size of $20 \times 20 \text{ cm}^2$ by the conventional spin-coating method. At first, the chloroform solution was spin-coated on a glass substrate with rubbed polyimide layer and heated up to the S_A temperature of 180°C . By this simple method, the homogeneously aligned S_A monodomain can be prepared. It was then cooled down to the S_C^* temperature of 120°C , annealed for 5 min , and solidified on further cooling to room temperature. In this monodomain film, the helical axes align uniaxially along the rubbing direction and parallel to the film surface, leading to the nanostructures working as a diffraction grating.⁸ In Figure 5 is shown such a film with a thickness of $5 \mu\text{m}$. It exhibits the beautiful reflection lights in a limited viewing angle. AFM image at any position of this film shows the perfectly aligned and equally spaced grooves (see the inset). Such monodomain S_C^* films give the opportunity to produce large area nanostructures at easy processing which could be applied to developing a new generation of optical and electronic devices.^{9–11}

Conclusion

In summary, microscopic analyses using FE-SEM and AFM revealed the sinusoidal undulation morphology on the fracture surface of chiral S_C^* solid. The peak to peak distance corresponds to the helical pitch of chiral S_C^* phase ($150\text{--}600 \text{ nm}$ depending on the chiral content in the polymers), and the depth from top to bottom is around $20\text{--}80 \text{ nm}$. Such an undulation

mode on the fracture surface results from the helical arrangement of polymers which are incorporated into the macrohelix of S_C^* ; the preferential direction of cleavage is along the helical polymer chain. The undulation morphology is also observed on the film surface of homogeneously aligned film although the depth, relatively smaller than that observed on the fracture surface, is around $5\text{--}10 \text{ nm}$. Interfacial tension may act to produce a more gentle undulation. This is the first report to show that the inner nanostructure can induce the surface nanostructuring.

Acknowledgment. This research was supported by the Grant-in-Aid for Creative Scientific Research from Ministry of Education, Science, Sports and Culture.

References and Notes

- (1) Goodby, J. W.; Blinc, R.; Lagerwall, L. A.; Osipov, M. A.; Pikins, S. A.; Sakurai, T.; Yoshino, K.; Zeks, B. *Ferroelectric Liquid Crystals; Principles, Properties and Applications*; Gordon & Breach Science Publishers: Paris, 1991.
- (2) Watanabe, J.; Hayashi, M.; Morita, A.; Tokita, M. *Macromolecules* **1995**, *28*, 8073.
- (3) Watanabe, J.; Hayashi, M.; Nakata, Y.; Niori, T.; Tokita, M. *Prog. Polym. Sci.* **1990**, *22*, 1053.
- (4) Watanabe, J.; Hayashi, M. *Macromolecules* **1989**, *22*, 4083.
- (5) Watanabe, J.; Hayashi, M.; Kinoshita, S.; Niori, T. *Polym. J.* **1992**, *24*, 597.
- (6) Watanabe, J.; Kinoshita, S. *J. Phys. II* **1992**, *2*, 1273.
- (7) Gray, G. W.; Goodby, J. W. *Smetic Liquid Crystals—Textures and Structures*; Leonard Hill: Glasgow, 1986.
- (8) Hutley, M. C. *Diffraction Gratings*; Academic Press: London, 1982.
- (9) Chou, S. Y.; Krauss, P. R.; Renstrom, P. J. *Appl. Phys. Lett.* **1995**, *67*, 3114.
- (10) Guo, L. J. *J. Phys. D* **2004**, *37*, R123.
- (11) Lee, W.; Jin, M.-K.; Yoo, W.-C.; Lee, J.-K. *Langmuir* **2004**, *20*, 7665.